Journal of the European Ceramic Society **18** (1998) 1235–1243

PII: S0955-2219(98)00048-X
0955-2219/98/$—see front matter

Zirconium Titanate: from Polymeric Precursors to Bulk Ceramics

Alessandra Bianco,[a]* Maurizio Paci[a] and Robert Freer[b]

[a]Dipartimento di Scienze e Tecnologie Chimiche, Universita' di Roma 'Tor Vergata', Via della Ricerca Scientifica, 00133 Rome, Italy
[b]Materials Science Centre, University of Manchester/UMIST, Grosvenor Street, Manchester, M1 7HS, UK

Abstract

Ceramic materials based on zirconium titanate solid solutions are used extensively in microwave telecommunications and catalysis. They also find applications in sensors, pigments, and composites. The preparation of zirconium titanates via polymeric precursors is reported. The behaviour of samples containing either no metallic component or a single metal component is also discussed. All the precursors were characterised by NMR, FT-IR and thermal analysis (DTA-TGA). Oxide powders were obtained by calcining the polymeric precursors at temperatures in the range 460–1200°C. The products were characterised by XRD, DTA, SEM and EDS. By sintering at 1600°C the zirconium titanate powders, dense (up to 98% theoretical density) $ZrTiO_4$ ceramics were obtained without additives. © *1998 Elsevier Science Limited. All rights reserved*

1 Introduction

The applications of ceramics based on zirconium titanate solid solutions are extremely wide. They range from microwave telecommunications (as capacitors, dielectric resonators in filters and oscillators,[1–3] to catalysis (as effective acid-base bifunctional catalysts[4]) and chemical industry (as high-temperature pigments[5]). Moreover, mixed oxides based on ZrO_2 and TiO_2 have found interesting applications in composites[6] and sensors.[7] Finally, the potential technological applications of $ZrTiO_4$ thin films in optics have recently been explored.[8]

In order to obtain fined grained, high quality electroceramic powders at low processing temperatures, various chemical routes have been developed as alternatives to the conventional solid state reaction route. The more popular chemical routes include the simultaneous hydrolysis of metal alkoxides,[9–11] synthesis of metallorganic salts,[12] the co-precipitation of metal salts from aqueous solutions,[13,14] preparation via sol–gel of reactive hydroxoperoxo compounds.[15] The preparation of mixed-cation oxides via polymeric precursors represents an attractive alternative route to those mentioned above. The main advantages are chemical homogeneity (segregation is prevented by the high viscosity), and versatility. Moreover, the gel can be deposited on substrate; subsequent ignition leaves a thin film of the required composition.[16,17]

$ZrTiO_4$ ceramics have the orthorhombic structure of α-PbO_2 and belong to the space group *Pbcn*.[18] On cooling within the temperature range 1200–1100°C, a sluggish disorder–order transition has been observed; the transition is accompanied by a slight volume decrease mostly due to the shortening of the *b* axis.[19] The distribution of cations within the lattice also changes: (i) in the 'high temperature' form (disordered) the metal ions are randomly distributed in the octahedral sites; (ii) in the 'low temperature' form (ordered) the alternation of two distorted Zr layers (8-coordinate) and two Ti layers (6-coordinate) gives rise to a doubled axis along the *a* direction.[20,21]

In this study, zirconium titanate powders have been obtained via polymeric precursors following a chemical route based on the Pechini process. In order to fully investigate their chemical structure and phase evolution during calcination, polymeric precursors containing either no metallic components (matrix) or a single metallic component have also been prepared. The chemical structure of the polymeric precursors, the distribution mode of the cations within the organic network, and the identification of their coordination sites were studied by

*To whom correspondence should be addressed.

means of infra-red spectroscopy, nuclear magnetic resonance and mass spectrometry; the thermal decomposition process of the polymeric precursors was followed by thermal analysis. The zirconium titanate powders, produced by calcination of the polymeric precursors at different temperatures, were studied by X-ray diffractometry, thermal analysis, scanning electron microscopy, and energy dispersive spectroscopy. Finally, preliminary results on sintered $ZrTiO_4$ ceramics are also reported.

2 Experimental Materials and Techniques

2.1 Materials

2.1.1 Polymeric precursors

The zirconium titanate (ZT) precursor was obtained by dissolving the following reagents in ethylene glycol: $Ti(OBut)_4$ (Aldrich 99%), $ZrOCl_2 \cdot 8H_2O$ (Aldrich 98%, Hf–0·5%), and citric acid. The weight ratio of ethylene glycol/citric acid was 60/40, the metallic precursors were in equimolar amounts, and their overall concentration was 1·5 M. The mixture was heated at 110°C until a viscous transparent gel was obtained. Using the same experimental conditions and chemicals, gels containing either no metallic components (matrix, M) or a single metallic component (titanium-based, T; zirconium-based, Z) were also prepared. Polymeric precursors were obtained by keeping the gels in an oven at 120°C for several days.

2.1.2 Ceramic powders

The Z, T, and ZT polymeric precursors were firstly baked at 300°C for 4 h and then calcined in air to give the oxide powders. The thermal treatment employed the following conditions: heating rate 120°C h^{-1}, dwell at peak temperature 2 h, furnace cooling to room temperature. Three different peak temperatures where used: $T = 460$°C, $T = 750$°C and $T = 1200$°C.

A typical preparation process of ceramic powders from polymeric precursors is illustrated in the block diagram reported in Fig. 1.

2.1.3 Sintered pellets

ZT ceramic powders (about 2 g) were uniaxially pressed at 100 MPa into 12 mm diameter pellets; green bodies were sintered at 1600°C for 4 h: heating and cooling rate 300°C h^{-1}.

2.2 Characterisation techniques

Viscosity measurements on the gels (Brookfield, Model DVII + Viscosimeter) were performed under the following conditions: beaker 100 ml, RPM 50, time 20 s, temperature 26·5°C, spindle S04.

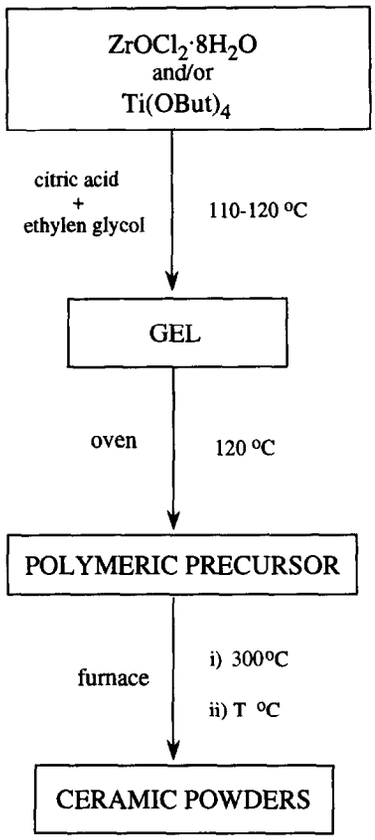

Fig. 1. Typical preparation process of ceramic powders via polymeric precursors.

FT-IR (Fourier transform infra-red) spectra (Perkin–Elmer System 2000 FT-IR) were collected in the range 6500–400 cm^{-1}, the samples being constrained as thin layers within CsI plates.

C-13 CPMAS NMR (cross polarisation magic angle spinning nuclear magnetic resonance) spectra were run with a Bruker instrument AM 400 operating at 100·6 MHz with a double bearing probe. The spectra were obtained in the following conditions: temperature 298 K; rotation 4200 Hz; contact time 1·2 ms.

Mass spectra (electron impact, E.I.) were collected on a VG QUATTRO (triple quadrupole) by solid probe inlet ($E = 70$ eV).

Differential and thermogravimetric thermal analysis (DTA-TGA) (Netzsch mod. STA 409) were performed using the following conditions: sample weights 60 mg (polymeric precursors)and 30 mg (ceramic powders); atmosphere air 80 cc min^{-1}; heating rates 2°C min^{-1} (polymeric precursors) and 10°C min^{-1} (ceramic powders).

X-ray diffraction (XRD) (SIEMENS) spectra for powders and sintered products were collected under the following conditions: CuK_α 1·5406 Å; range $2\theta = 20$–80.

Lattice parameters of the orthorhombic cell of $ZrTiO_4$ were determined from the (110), (111), (020) and (002) reflections by profile fitting and iterative calculations. The microstructures of powders and ceramics were investigated by scanning

electron microscopy (SEM, Leica, Cambridge, mod. Stereoscan 360); the elements present were identified by energy dispersive spectroscopy (EDS) (Link EXL II).

The densities of green and sintered specimens were determined from weight and dimension measurements.

3 Results and Discussion

3.1 As-prepared gels and polymeric precursors

3.1.1 M, Z, T and ZT as-prepared gels: viscosity, FT-IR

The viscosities of the gels were the range 3400–3600 cp. The FT-IR measurements were run on all the as-prepared gels; in Fig. 2 the spectra of M and ZT gels are compared. All the spectra are the same between 4000 and 2000 cm^{-1}, where the bands related to the stretching mode of O–H and H–C–H of the diol are found. In the region from 2000 to 1500 cm^{-1}, where there are no peaks from ethylene glycol and titanium tetrabutoxide, the spectra are dominated by the band of (O–)C=O stretching typical of carboxy groups. In the case of the M gel, only a single sharp peak at 1736 cm^{-1} is detected [Fig. 2(a)]; gels containing either one (Z and T) or two metallic precursors (ZT) showed in this range a multiple peak. In particularly, three peaks were observed at 1736 cm^{-1}, 1654 cm^{-1} and 1560 cm^{-1} [Fig. 2(b)]. The first absorption band was assigned to the C=O of the carboxylic acid and/or to the ester formed by polycondensation; the second and the third ones are attributed to the stretching mode of the carboxylic group for a monodentate and bidentate complex to metal cations, respectively.[22] Between 1500 and 1200 cm^{-1} the spectra are not significantly different. At lower wavenumbers, in all the spectra several bands characteristic of linear polyols can be easily recognised (1084 and 1040 cm^{-1} C–O stretching; 880 cm^{-1}, C–C stretching). Finally, in the case of Z, T and ZT gels the peak at 622 cm^{-1} corresponds the oxygen–metal/s stretching mode, as can be deduced by the FT-IR spectra of the Z and T gels.

3.1.2 Solid matrix and polymeric precursors: C-13 CPMAS NMR

The technique allows monitoring of the physical state of the solid samples at molecular level, being sensitive to the microcrystallinity and to the homogeneity of chemical composition. Recently, C-13 NMR studies of polymeric precursors obtained by analogous procedures have been reported for $SrTiO_3$[22] and $BaTiO_3$.[23]

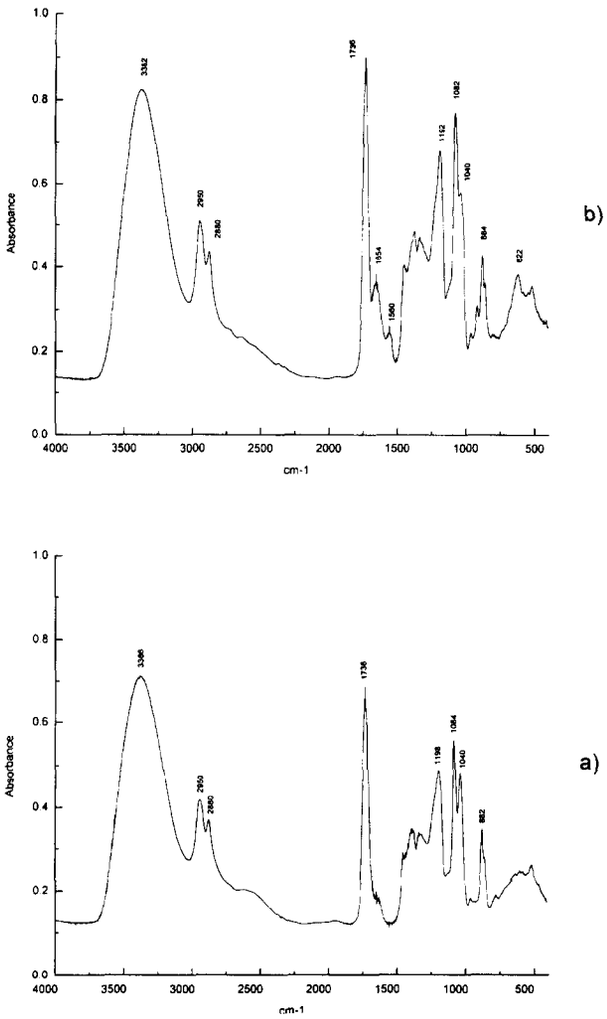

Fig. 2. FT-IR spectra of as-prepared gels (a) M and (b) ZT.

The spectra of the solid matrix (M) and of the Z, T and ZT polymeric precursors are shown in Fig. 3. The resonances, due to the carbon atoms present in the polymeric precursors are listed in Table 1. The spectrum of M is shown in Fig. 3(a), the resonance of the carboxy group (–COO) at 170 ppm is clearly visible. The group of resonances between 60 and 80 ppm are assigned to the methylene carbons (–CH_2–) of the ethylene glycol. The peak at 44 ppm is assigned to the methylene carbons of the citric acid. The multiple resonances in the range 60–80 ppm are due to the different physical environments where the methylene carbons are located. The very sharp peak at 74 ppm is likely to be due to the reaction of ethylene glycol with citric acid only by one of the hydroxy groups. The other resonances at 68 and 66 ppm are probably due to the reaction of ethylene glycol by both the hydroxy groups and at the central carboxyl group of citric acid, respectively. The broadness of the resonance at 44 ppm is due to the different environment of the two nearby carboxyl groups. The presence of Zr in the reaction mixture markedly changes the spectrum [Fig. 3(b)]. Firstly, it displays a shoulder downfield with respect to the 170 ppm resonance

Table 1. Assignment of the resonances of the C-13 CPMAS NMR spectrum (Fig. 2) of the solid matrix (M) and of the Z, T and ZT polymeric precursors

Sample	*C(OO) citrate (180–170 ppm)*	*CH_2–(O) ethylene glycol (85–60 ppm)*	*(C)–CH_2–(COO) citrate (44–45 ppm)*
		74	
M	170	68	44 (broad)
		66	
		80	
	178	74	
Z	170	70(b)	44 (sharp)
		68	
		64	
		85	
	183	74	
T	170	68	44 (sharp)
		66	
		62	
	183	85	
	178	80	
ZT	170	74	44 (sharp)
		68	
		64	
		62	

that is clearly due to the resonance of those carboxyl groups bonded with the metal cations. Secondly, the peak at 80 ppm is attributed to ethylene glycol molecules coordinated to metal cations by both the hydroxyl groups; the broad shoulder-like peak at approximately 70 ppm indicates that salt bridges are also formed. Finally, a new broad resonance at 64 ppm is also present; this is attributed to those methylene groups linked to the metal cation on one side and to citrate on the other one. The narrowness of the 44 ppm resonance of the citrate methylene carbons is due to a decrease of multiplicity of the environments around these carbons. This clearly indicates that the central carboxyl groups are almost completely involved in the formation of salt bonds with the metal cations. In the presence of Ti (see spectrum *c* in Fig. 3), two new broad shoulders appears downfield with respect to both the 170 ppm and the 74 ppm resonances; their assignments are analogous to those reported in the case of Z [Fig. 3(b)]. Moreover, the lack of the broad resonance around 70 ppm clearly indicates that no salt bridges are formed with ethylene glycol. The three sharp resonances at 68, 66 and 62 ppm are characteristic of self-polymerized ethylene glycol. The assignment of the sharp resonance at 44 ppm is analogous to that reported in the case of Z sample. Finally, spectrum *d* in Fig. 3 shows that reaction in the presence of both Zr and Ti metals gives rise to a solid state spectrum that is nearly the sum of the two individual spectra. The only difference seems to be the lack of the broad resonance at 70 ppm (spectrum *b*) indicating that in the ZT polymeric precursor no salt bonds are formed between metal cations and ethylene glycol.

In conclusion, the comparison between the solid state spectra yields: (i) information on the structure of the organic matrix itself and in presence of the metallic component/s; (ii) identification of coordination sites of metal cations. In particular, the matrix (M) can be described as a disordered solid [see broadness of the peak at 44 ppm in Fig. 3(a)]; the polycondensation between citric acid and ethylene glycol produces a rigid network in which the mono-esterified form of the polyol is prevalent [see in Fig. 3(a) the relative intensity of the peaks at 74 and 68 ppm]. In the presence of the metallic cation/s, the solid acquires a certain degree of order (see the sharpening of the resonance at 44 ppm), indicating that no separate domains containing single metallic species are present within the polymer. Moreover, in both the T and ZT samples a partial self-polymerisation of ethylene glycol is also observed. In the T polymeric precursor, most of the Ti cations are coordinated with the carboxyl groups; in the Z polymeric precursor, Zr cations also form salt bonds with the glycol. It is likely that this is responsible for the distinct macroscopic

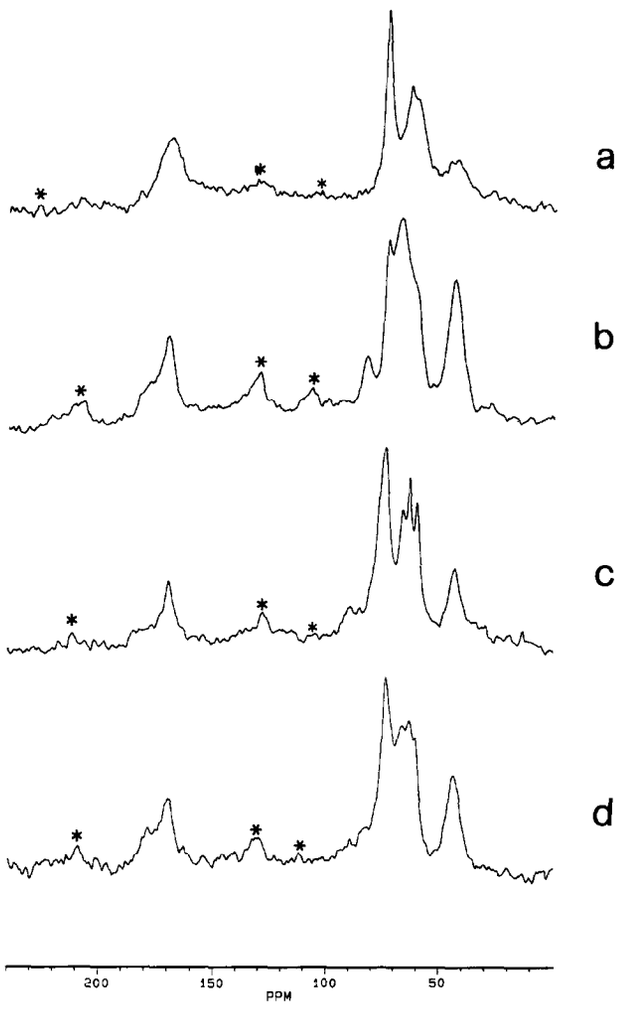

Fig. 3. C-13 CPMAS NMR spectra of the polymeric precursors (a) M, (b) Z, (c) T and (d) ZT.

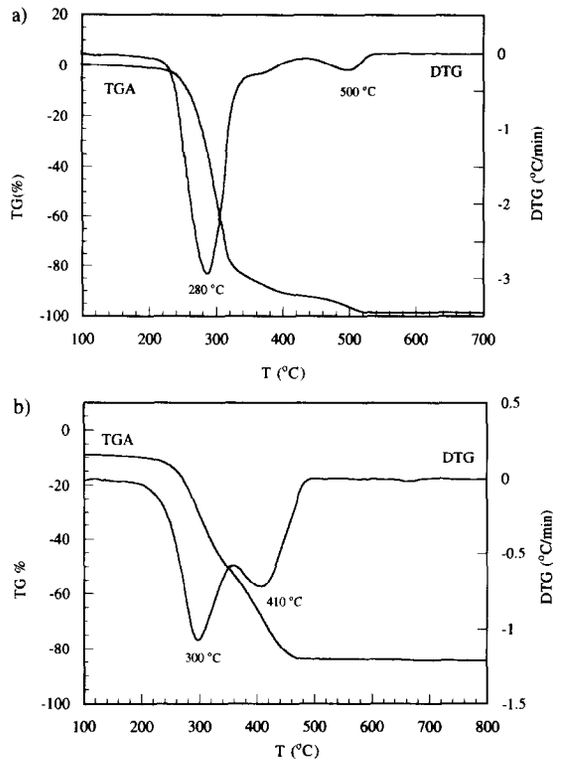

Fig. 4. TGA and DTG curves of the polymeric precursors (a) M and (b) ZT.

aspect of the Z polymeric precursor (opaque, whitish, brittle) with respect to the M, T and ZT polymeric precursor (transparent, yellowish-red, hard). In the case of the ZT polymeric precursor it was found that (i) no salt bonds are formed between metal cations and ethylene glycol; (ii) Zr and Ti cations are coordinated to the carboxyl groups, information on the coordination mode being provided by the FT-IR (see above).

3.1.3 Thermal behaviour

The thermal decomposition of polymeric precursors was studied by thermal analysis; additional information was also obtained by mass spectrometry.

The matrix was completely burnt out by 540°C. The process develops in two steps [Fig. 4 (a)]: the 95% of the weight is decomposed below 350°C; the residual part decomposes at higher temperatures (460–530°C). The Z,T, and ZT samples [Fig. 4(b)] were totally decomposed by 460°C; for all samples, the weight loss ranged between 80 and 90%. It is worthwhile noting that ZT polymeric precursors obtained by a similar procedure are totally decomposed only at 600°C.[24]

The kinetics of the burning process was studied by DTG curves (Fig. 4). For the T and ZT precursors that a two-step combustion process occurred: first minimum at 230 and 300°C, respectively; second one at 300 and 410°C, respectively. Only the Z precursor followed a single step process, the minimum on the DTG curve being at 240°C. This characteristic kinetics of combustion could be associated with the presence of zones of poly-ethylene glygol (PEG) (see NMR results) within the T and ZT polymers, possibly due to the presence of 55% wt excess of ethylene glycol (with respect to the citric acid).

The difference in thermal stability between the solid matrix (M) and the polymeric precursors containing either one or two metallic component (T, Z, and ZT) (Fig. 4) can be attributed to their distinct chemical structures. In fact, as discussed above (see NMR results), the matrix is more reticulated than the polymer containing the metallic precursor/s. In particular, the presence of the excess of ethylene glycol (with respect to citric acid) induced the prevalence of the esterification by one of the hydroxyl groups; addition of $Ti(OBut)_4$ and/or $ZrOCl_2$ caused the subtraction of functional sites to the polycondensation process, producing a more 'open' structure, less thermally resistant with respect to the matrix. In order to substantiate these results, mass spectrometry was performed on all

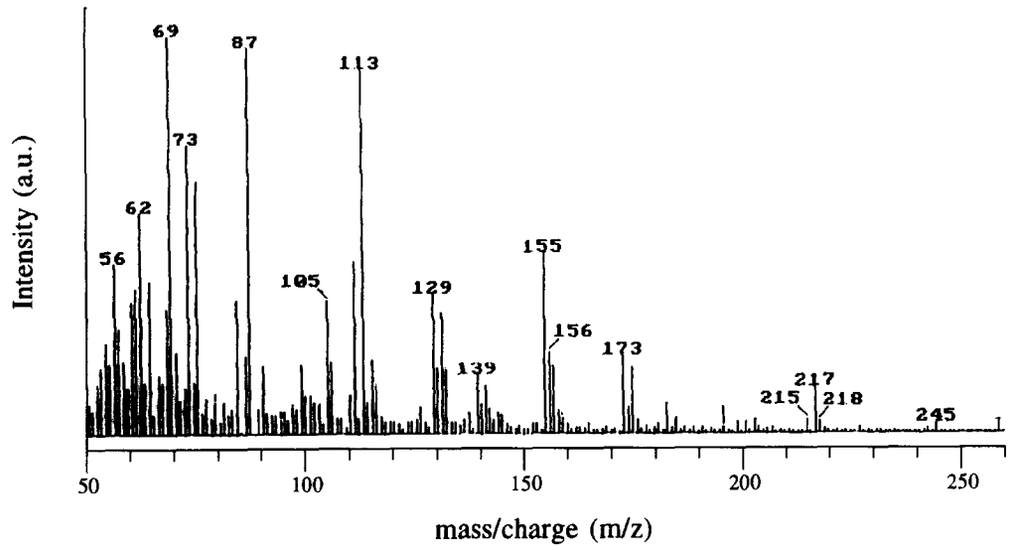

Fig. 5. Mass (EI^+) spectrum of the matrix (M).

the precursors. In the case of T, Z and ZT samples, no significant peaks were found at higher mass/charge (m/z) than 139. For M, the presence of peaks at m/z 245, 217, 173, and 155 showed that 8–9 carbon rings are also present within the network (Fig. 5).

3.2 Ceramic powders

3.2.1 Phase formation

T, Z and ZT ceramic powders were obtained by calcination of the T, Z, and ZT polymeric precursors 460°C, after being pre-heated at 300°C. EDS analysis revealed that the latter Z and ZT samples were, at this stage, free of Cl and, in the ZT sample, Zr and Ti are uniformly distributed.

XRD spectra showed that the ZT powder was amorphous whilst the T and Z powders were already crystallised as metastable phases. The T and Z spectra are shown in Fig. 6. In particular, titanium oxide is present as both rutile (JC-PDS 21-1276) and anatase (JC-PDS, 21-1272), one small extra peak (indicated by an asterisk) is also detected;[22] zirconium oxide crystallises in the orthorhombic form (JC-PDS 37-1413). DTA measurements (up to 1200°C) of ZT and Z samples showed an exothermic transformation without weight change around 700°C; in the case of the T sample no peaks were detected. The DTA curve for the ZT sample is shown in Fig. 7. ZT polymeric

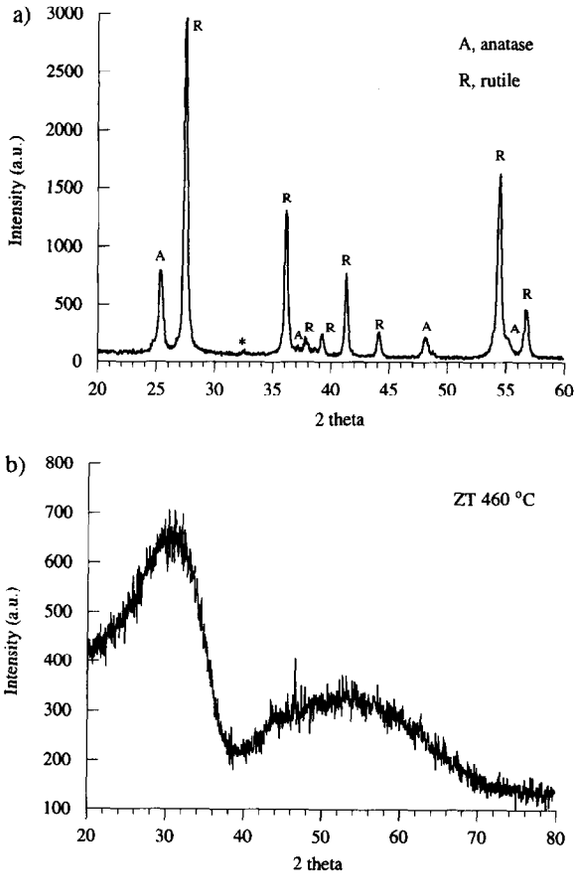

Fig. 6. XRD spectra of the powder obtained calcining the (a) T and (b) ZT polymeric precursors at 460°C.

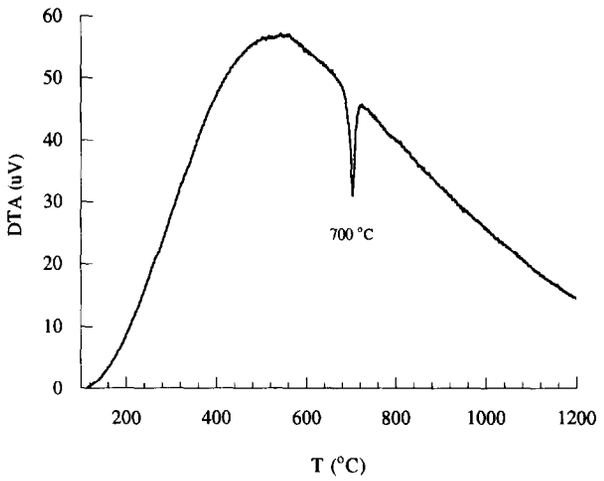

Fig. 7. DTA curve of the powder obtained calcining the ZT precursor at 460°C.

precursors have thus been calcined at 750°C, the XRD spectrum is reported in Fig. 8 (a). The pattern analysis showed that the crystallisation of $ZrTiO_4$ occurred (JC-PDS 34-415).[10] Most of the zirconium titanate powders obtained by chemical routes crystallise around 700°C.[11,25,26] In recent studies, $ZrTiO_4$ powders have been also obtained at temperature as low as 500°C[27] and 300°C.[12]

In order to study the phases present above the disorder–order transition phase temperature (around 1120°C), the ZT polymeric precursor was fired at 1200°C. To provide a full picture of the phase evolution with temperature and to investigate for the distinctive DTA results reported above, Z and T polymeric precursors were also calcined at 1200°C and furnace cooled to room temperature. For the Z and T samples, baddeleyite (JC-PDS, 37-1484) [Fig. 9 (a)] and rutile [Fig. 9(b)] phases were found, respectively; in both spectra small additional peaks (indicated by an asterisk) were also observed. These results clearly explain the DTA profiles described above.

For the ZT sample the 'high temperature' (disordered) form of $ZrTiO_4$ was identified

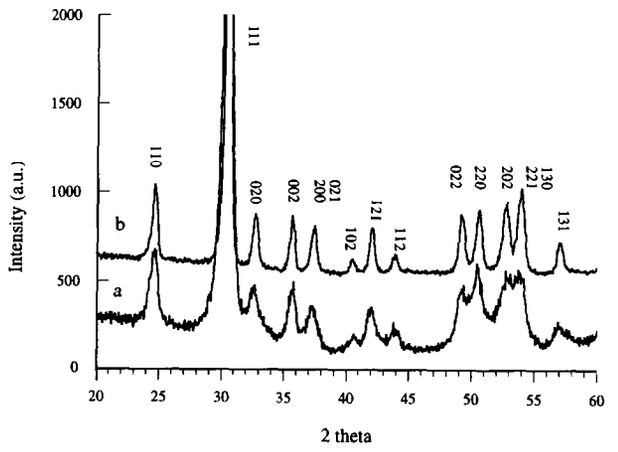

Fig. 8. XRD spectra of the powder obtained calcining the ZT precursor at (a) 750°C and (b) 1200°C.

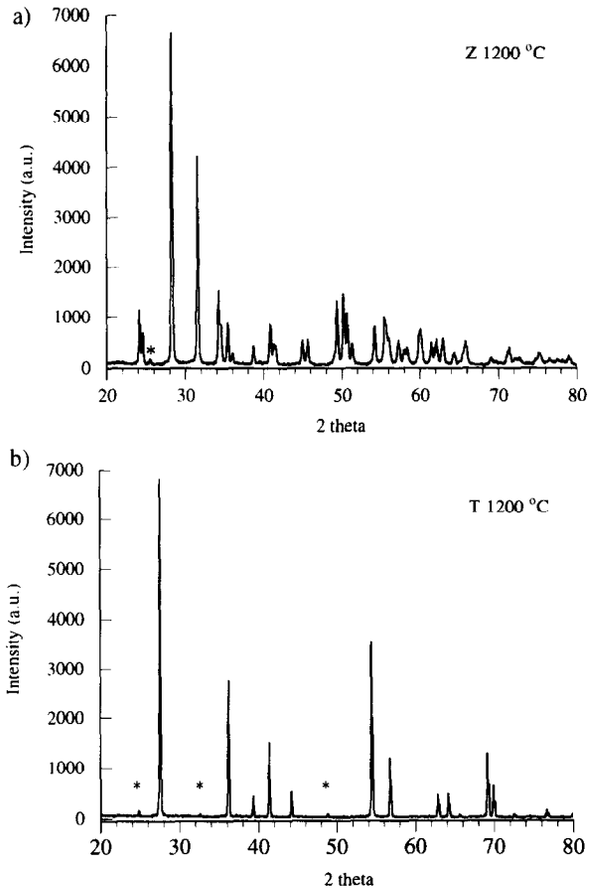

Fig. 9. XRD spectra of the powder obtained calcining the (a) Z and (b) T polymeric precursors at 1200°C.

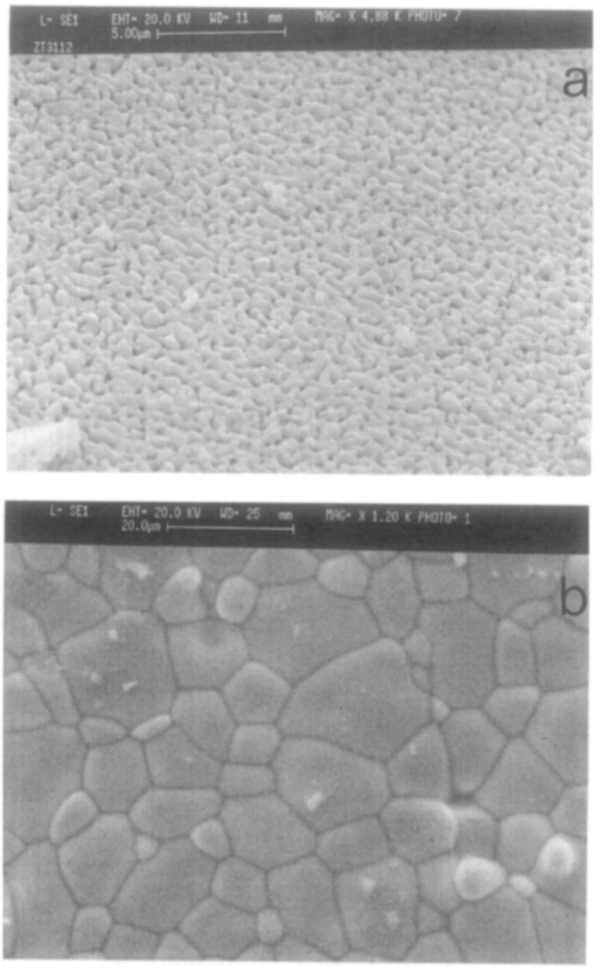

Fig. 10. SEM micrographs of (a) $ZrTiO_4$ powder obtained calcining the ZT polymeric precursors at 1200°C; (b) as-sintered $ZrTiO_4$ pellet.

[Fig. 8(b)]; the calculated cell parameters of the orthorhombic cell are $a = 5{\cdot}036$ Å, $b = 5{\cdot}453$ Å and $c = 4{\cdot}794$ Å.

3.2.2 Microstructure of $ZrTiO_4$ powders

A distinct resolved microstructure can only be clearly observed by SEM for powders obtained by high temperature calcination (i.e. above 1000°C). As shown in Fig. 10(a), the samples are characterised by very uniform microstructure. SEM studies performed at higher magnification showed that the powders were made up of agglomerated sub-micronic spherical particles. The agglomeration is due to the large heat of combustion developed during the thermal decomposition process. EDS maps for Zr and Ti showed that Zr and Ti are uniformly distributed within the samples.

3.3 Sintered pellets

3.3.1 Phase and microstructure

Bulk ceramics were produced by sintering uniaxially-pressed pellets without additives or binder. The density of green bodies was around 60% of the theoretical value. The density of sintered pellets range from 85 to 98% of the theoretical value, depending on the calcination temperature of the precursor (460, 750 and 1200°C). The surfaces of as-sintered pellets are made up of polygonal grains (5–20 μm); only few small pores are visible, mostly at the triple point positions [Fig. 10(b)]. Hirano *et al.*[9] obtained ZTS bulk materials with similar microstructure by sintering zirconium titanate powders obtained by the controlled hydrolysis of metal alkoxides. All the peaks in the XRD spectra (Fig. 11) were indexed against $ZrTiO_4$, except for the extra peaks indicated by an asterisk. It is likely that the latter represents one of the low

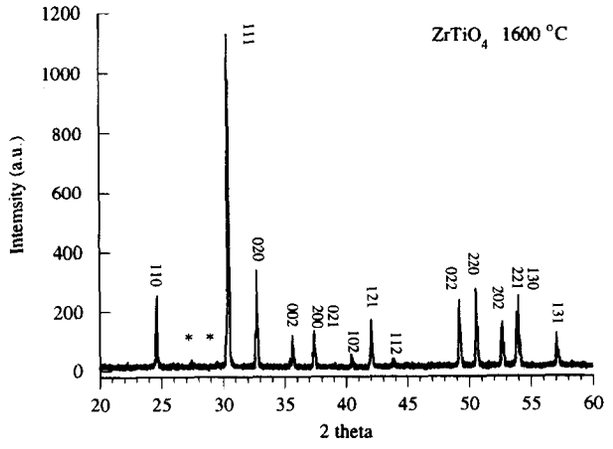

Fig. 11. XRD spectrum for a sintered $ZrTiO_4$ pellet.

angle superlattice reflections of the 'low temperature' (ordered) form of zirconium titanate the cooling rate (300°C h^{-1}) through the disorder–order transition being was too fast to enable the ordered form to fully develop. However, detailed XRD measurements and TEM studies are needed to confirm this point.[28,29]

4 Conclusions

Zirconium, titanium and zirconium titanate polymeric precursors were prepared from citric acid, ethylene glycol, titanium tetrabutoxide and/or zirconium oxychloride. The 'parent' matrix was also prepared by the same experimental conditions. IR and NMR results suggested that the zirconium titanate precursor can be described as a disordered solids, the metallic cations being mostly coordinated to the carboxyl groups and uniformly dispersed within the network. In the case of the organic matrix a more reticulated structure was found. The combustion process of all the precursors was studied by thermal analysis. It was found that the organic component present in the polymeric precursors containing the metallic component/s was totally decomposed by 460°C, with an associated weight loss of 80–90%. The organic matrix was totally burned out at higher temperatures (530°C). In the case of the precursors containing only a single metallic component, XRD showed that at 460°C metastable phases of zirconium dioxide and titanium dioxide were already formed. The crystallisation of zirconium titanate in the metastable 'high temperature' form (disordered) occurred around 700°C. This temperature was much lower than the processing temperature needed to obtain single phase zirconium titanate by solid state reaction (1200–1400°C). In order to study the phase evolution above the disorder–order transition temperature, the precursors were also calcinated at 1200°C. The phase present in the Z, T and ZT samples were baddeleyite, rutile and zirconium titanate, respectively. Finally, sintering the ZT powders at 1600°C, dense $ZrTiO_4$ pellets (up to 98% theoretical density) were produced without the use of any additive. However, in the latter case it was not possible to confirm definitively that partial conversion to the ordered form had effectively occurred. Detailed XRD and TEM measurements are needed to clarify this point.

Acknowledgements

The authors wish to thank Professor G. Gusmano for the opportunity to perform this work in his laboratories and Professor T. Boschi and Mr G. D'Arcangelo for the mass spectrometry measurements. This work has been partially supported by the British Council (British–Italian Collaboration in Research and Higher Education).

References

1. Wakino, K., Minai, K. and Tamura, H., Microwave characteristics of (Zr,Sn)TiO_4 and BaO–PbO–Nd_2O_3–TiO_2 dielectric resonators. *J. Am. Ceram. Soc.*, 1984, **67**, 278–281.
2. Osbond, P. C., Whatmore, R. W. and Ainger, F. W., The properties and microwave applications of zirconium titanium stannate ceramics. *Proc. Br. Ceram. Soc.*, 1985, **36**, 167–178.
3. Moulson, A. J. and Herbert, J. M., *Electroceramics*. Chapman and Hall, London, 1990, p. 239.
4. Daly, F. P., Ando, H., Schmitt, J. L. and Sturm, E. A., *J. Catal.*, 1987, **108**, 401–408.
5. Hund, F., $ZrTiO_4$—mixed phase pigments (in German). *Z. Anorg. Allg. Chem.*, 1985, **525**, 221–229.
6. Parker, F. J., Al_2TiO_5–$ZrTiO_4$–ZrO_2 composites: a new family of low-thermal-expansion ceramics. *J. Am. Ceram. Soc.*, 1990, **73**, 929–932.
7. Yang, S. and Wu, J. M., *J. Mat. Sci.*, 1991, **26**, 631–636.
8. Chang, D.-A., Lin, P. and Tseng, T., Optical properties of $ZrTiO_4$ films grown by radio-frequency magnetron sputtering. *J. Appl. Phys.*, 1995, **77**, 4445–4447.
9. Hirano, S., Hayashi, T. and Hattori, A., Chemical processing and microwave characteristics of (Zr,Sn)TiO_4 microwave dielectrics. *J. Am. Ceram. Soc.*, 1991, **74**, 1320–1324.
10. McHale, A. E. and Roth, R. S., Low-temperature phase relationship in the system ZrO_2–TiO_2. *J. Am. Ceram. Soc.*, 1986, **69**, 827–832.
11. Yamaguchi, O. and Mogi, H., Formation of zirconia titanate solid solution from alkoxides. *J. Am. Ceram. Soc.*, 1989, **72**, 1065–1066.
12. Sekar, M. M. A. and Patil, K. C., Hydrazine carboxylate precursors to fine particle titania, zirconia and zirconium titanate. *Mat. Res. Bull.*, 1993, **28**, 485–492.
13. Ikawa, K., Iwai, A., Hiruta, K., Shiimojima, H., Urabe, K. and Udagawa, S., Phase transformation and thermal expansion of zirconium and hafnium titanates and their solid solutions. *J. Am. Ceram. Soc.*, 1988, **71**, 120–127.
14. Krebs, M. A. and Condrate, R. A.Sr, A Raman spectral characterisation of various crystalline mixtures in the ZrO_2–TiO_2 and HfO_2–TiO_2 systems. *J. Mat. Sci. Lett.*, 1988, **7**, 1327–1330.
15. Navio, J. A., Marchena, F. J., Macias, M., Sanchez-Soto, P. J. and Pichat, P., Formation of zirconium titanate powder from a sol-gel prepared reactive precursor. *J. Mat. Sci.*, 1992, **27**, 2463–2467.
16. Lessing, P. A., Mixed-cation oxide powders via polymeric precursors. *Ceram. Bull.*, 1989, **68**, 1002–1007.
17. Pechini, M. P., Method of preparing lead and alkaline earth titanates and niobates and coating using the same to form a capacitor. United States Patent. No. 3330697, 11 July 1967.
18. Newnham, R. E., Crystal structure of $ZrTiO_4$. *J. Am. Ceram. Soc.*, 1967, **50**, 216.
19. Bordet, P., McHale, A., Santoro, A. and Roth, R. S., Powder neutron diffraction study of $ZrTiO_4$, $Zr_5Ti_7O_{24}$ and $Fe_2Nb_2O_6$. *J. Solid State Chem.*, 1986, **64**, 30–46.
20. Christoffersen, R. and Davies, P. K., Structure of commensurate and incommensurate ordered phases in the system $ZrTiO_4$–$Zr_5Ti_7O_{24}$. *J. Am. Ceram. Soc.*, 1992, **75**, 563–569.
21. Yamamoto, A., Yamada, T., Ikawa, H., Fukunaga, O., Tanaka, K. and Marumo, F., Modulated structure of zirconium titanate. *Acta Cryst.*, 1991, **C47**, 1588–1591.

22. Leite, E. R., Sousa, C. M. G., Longo, E. and Varela, J. A., Influence of polymerisation on the synthesis of $SrTiO_3$: Part I. Characteristics of the polymeric precursors and their thermal decomposition. *Ceramics International*, 1995, **21**, 143–152.
23. Arima, M., Kakihana, M., Nakamura, Y., Yashima, M. and Yoshimura, M., Polymerized complex route to barium titanate powders using barium-titanium mixed-metal citric acid complex. *J. Am. Ceram. Soc.*, 1996, **79**, 2847–2856.
24. Cerqueira, M., Nasar, R. S., Longo, E., Leite, E. R. and Varela, J. A., Synthesis of ultra-fine crystalline $Zr_xTi_{1-x}O_4$ powders by polymeric precursor method. *Mat. Lett.*, 1995, **22**, 181–185.
25. Macias, M., Sanchez-Soto, P. J. and Navio, J. A., Kinetic study of crystallisation in zirconium titanate from an amorphous reactive prepared precursor. *J. Non-Crystalline Solids*, 1992, **147–148**, 262–265.
26. Khairulla, F. and Phule, P., Chemical synthesis and structural evolution of zirconium titanate. *Mat. Sc. and Engineering*, 1992, **B12**, 327–336.
27. Bhattacharya, A., Mallick, K., Hartridge, A. and Woodhead, J., Sol gel preparation and thermal stability of crystalline zirconium titanate microspheres. *J. Mat. Sci.*, 1996, **31**, 267–271.
28. Park, Y., Influence of order-disorder transition on microwave characteristics of tin-modified zirconium titanate. *J. Mat. Sci. Lett.*, 1995, **14**, 873–875.
29. Azough, F., Freer, R., Wang, C. -L. and Lorimer, G. W., The relationship between the microstructure and microwave properties of zirconium titanate ceramics. *J. Mat. Sci.*, 1996, **31**, 2539–2549.